Article

Tough, Long-Term, Water-Resistant, and Underwater Adhesion of Low-Molecular-Weight Supramolecular Adhesives

Xing Li, Yan Deng, Jinlei Lai, Gai Zhao, and Shengyi Dong

J. Am. Chem. Soc., **Just Accepted Manuscript** • DOI: 10.1021/jacs.0c00520 • Publication Date (Web): 24 Feb 2020

Tough, Long-Term, Water-Resistant, and Underwater Adhesion of Low-Molecular-Weight Supramolecular Adhesives

Xing Li,[a] Yan Deng,[a] Jinlei Lai,[a] Gai Zhao,[b]* and Shengyi Dong[a]*

[a]College of Chemistry and Chemical Engineering, Hunan University, Changsha, Hunan 410082, P. R. China

[b]State Key Laboratory of Mechanics and Control of Mechanical Structures, Nanjing University of Aeronautics and Astronautics, Nanjing 210016, P. R. China.

Supporting Information Placeholder

ABSTRACT: Modern functional adhesives have attracted considerable attention due to their reversible adhesion capacities and stimuli-responsive adhesion behavior. However, for modern functional adhesives, polymeric structures were highly necessary to realize adhesion behaviors. Supramolecular adhesives from low-molecular-weight monomers were rarely recognized. Compared with polymeric adhesive materials, it remains challenging for supramolecualr adhesive materials to realize tough adhesion on wet surfaces, or even under water. In this study, a new supramolecular adhesive consisting of low-molecular-weight monomers was successfully designed and prepared. Strong and long-term adhesion performance was realized on various surfaces, with a maximum adhesion strength of 4.174 MPa. This supramolecular adhesive exhibits tough and stable adhesion properties in high-moisture and underwater environments (including seawater). Long-term underwater adhesion tests display the potential application of low-molecular-weight adhesive as a marine adhesive.

INTRODUCTION

Tough adhesion on various surfaces is a remarkable feature of modern functional adhesives.[1,2] From conventional resins[3,4] and gums[5,6], to bio-inspired adhesive hydrogels[7-10], polymeric structures play a significant role not only in exhibiting excellent and long-term adhesion performances, but also in realizing adhesion behavior in special environments, e.g. high-moisture environments, or underwater.[11-15] For example, catechol-based adhesives represent a new type of modern adhesive with versatile adhesion applications.[16-21] At present, most underwater adhesives are based on the catechol structures. Wilker,[22,23] Stewart,[24,25] Dhinojwala,[26,27] and Lee[28,29] have independently reported many novel catechol-based polymeric adhesive materials, which exhibited excellent adhesion effects and were applicable under various conditions. However, by analyzing the chemical structures of catechol-based adhesive materials, it is reasonable that the realization of strong adhesion performances of catechols is crucially dependent on the polymeric structures.

Compared with the rapid development of polymeric adhesive materials, supramolecular adhesives assemblied from low-molecular-weight monomers were rarely recognized. In the past decade, with the development of supramolecular self-assembly, only a limited number of low-molecular-weight monomers (LMWMs) were used to construct supramolecular adhesives.[30-32] The versatility of supramolecular self-assembly has promoted significant efforts focused on supramolecular adhesion.[2,32-34] The combination of LMWMs and supramolecular self-assembly gives rise to supramolecular adhesives with reversible adhesion capacities and stimuli-responsive adhesion behaviors, which are not easily achieved in traditional polymeric adhesive systems.[32,35,36] However, most supramolecular adhesives consisting of LMWMs are not water-resistant and/or water dramatically attenuates the adhesion effect.[36,37] The water-sensitive adhesion properties of LMWMs significantly hinder the functionalization and further development of supramolecular adhesives.[36-38] Compared with the strong adhesion behaviors of polymeric adhesive materials under water, adhesion on wet surfaces is highly challenging for supramolecular adhesives consisting of LMWMs. There is an increasingly urgent demand to develop water-resistant, moisture insensitive or underwater supramolecular adhesives from low-molecular-weight monomers.

Here we report a new supramolecular adhesive, that exhibits strong and long-term adhesion effects on diverse surfaces, from hydrophilic glass and iron, to highly hydrophobic polytetrafluoroethylene (PTFE) and poly(methyl methacrylate) (PMMA). The non-viscous building blocks dibenzo-24-crown-8 (**DB24C8**) were rationally incorporated into a four-armed pentaerythritol (Scheme 1). Compared with individual **DB24C8** or pentaerythritol, supramolecular adhesive **P1** has a lower melting point (52 ºC) and shows excellent adhesion performance, which make **P1** an ideal candidate for a hot molten glue.[32] Tough adhesion of **P1** in a high-moisture (relative humidity, >95 RH%) environment or under water was successfully realized. Long-term adhesion in water or seawater (>12 months) is feasible due to the hydrophobic properties of **P1**.

RESULTS AND DISCUSSION

Characterizations and mechanical properties. P1-P4 were easily prepared *via* esterification reactions as shown in Scheme 1 and Figure S1-18. Owing to the low melting point (52 °C), **P1** is conveniently converted to a highly viscous liquid upon slight

heating (Figure 1a). In contrtast, **P3** and **P4** are oily liquids at room temperature. After cooling, **P1** transforms into an amorphous glue, according to the powder x-ray diffraction patterns (PXRD, Figure S21). Scanning electron microscopy (SEM) tests showed that there were no holes or fibers in the surface of **P1** (Figure S22, S25), supporting a high-density morphological structure.[36,37] The decomposition temperature of **P1** was measured by thermogravimetric analysis (TGA) to be 370 °C (Figure S30), indicating that **P1** is highly thermo-stable. No decomposition phenomena of **P1** were observed in water, acid

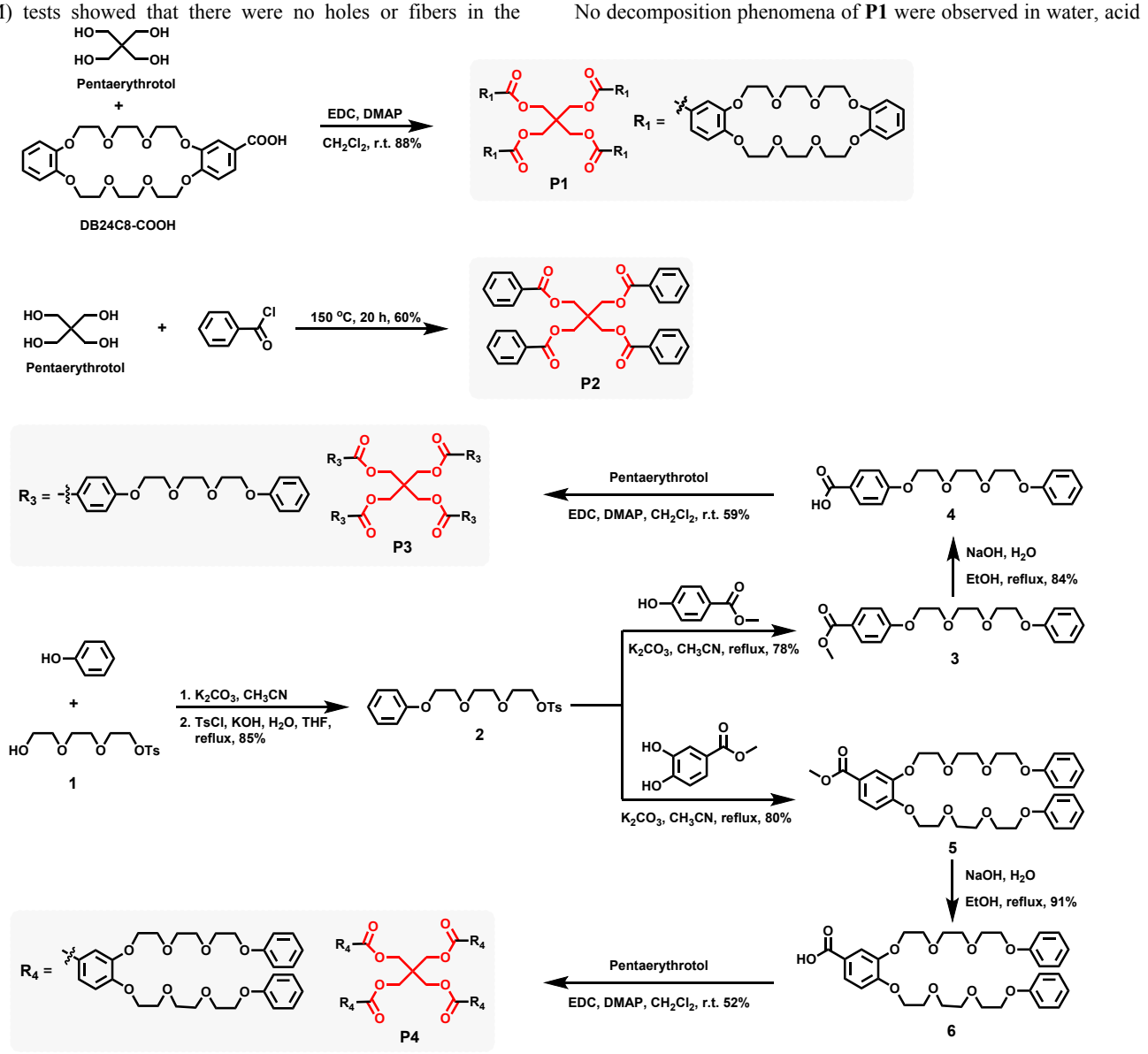

Scheme 1. Synthetic routes of **P1**, **P2**, **P3**, and **P4**.

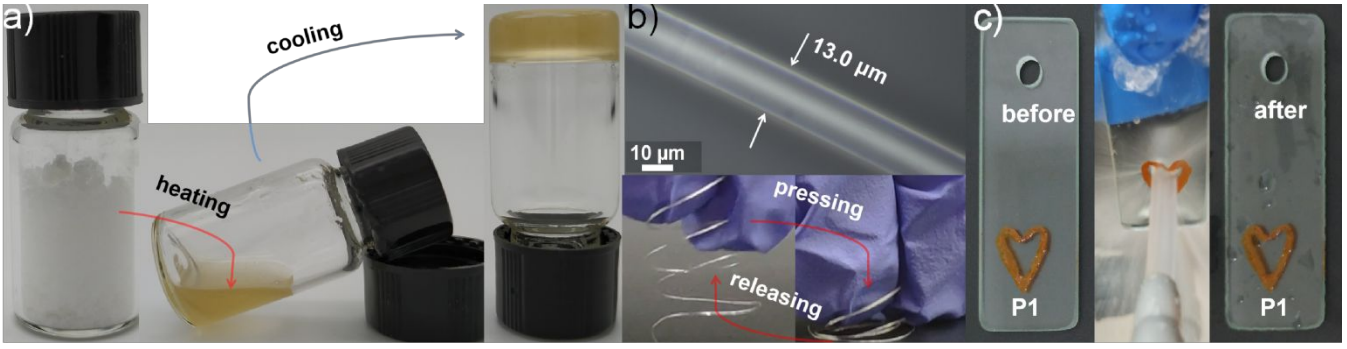

Figure 1. Macroscopic view of **P1**: a) glassy solid, fluid liquid after heating, and gel-like glue after cooling; b) a rod-like fiber and an elastic spring made of **P1**; c) water blasting (2 bars, 10 min) tests of **P1**. For Figure 1c, a dye was mixed with **P1** to get a clear view.

(2N HCl), base (2N NaOH) or under UV irradiation (254/365 nm, 20 W), after 12 months of treatment (Figure S31-34), which further confirm the environmental stability of **P1**.

After the heating-cooling cycle, **P1** showed good processability. Long and smooth fibers were mechanically pulled out from **P1**, and further processed into a spring (Figure 1b and movie S1). Thin (~100 μm), flexible (bending >180°), and transparent (>95% transmittance) membranes were also cast (Figure S23 and movie S2). Only short and rigid fibers were obtained from **P2**, and membrane formation was possible. In contrast, neither fibers nor

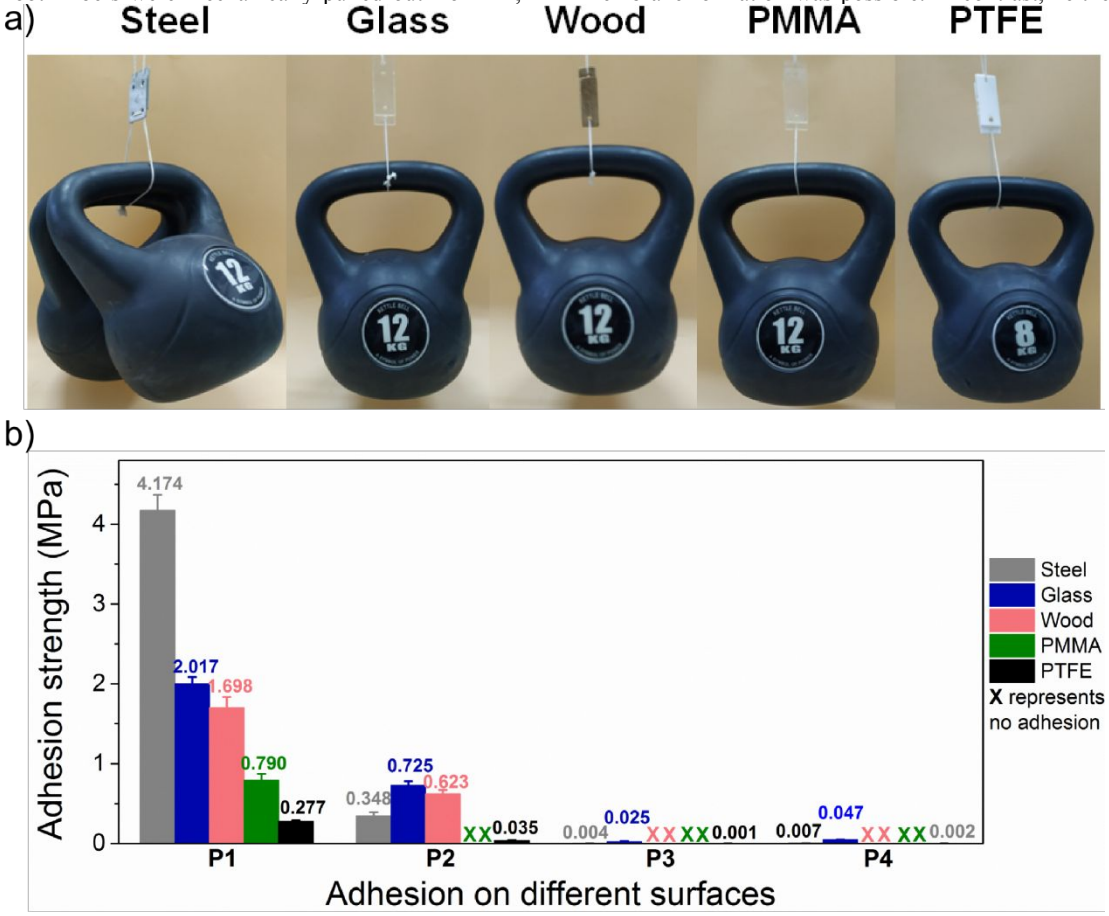

Figure 2. a) Macroscopic tests of adhesives on different substrates (adhesion areas are 15 cm^2, 18 cm^2, 9 cm^2, 18 cm^2, and 9 cm^2, respectively); b) the adhesion strengths of different adhesives on different substrates. Tests in Figure 2b were all carried out at 25 °C and 50 RH%.

membranes were successfully fabricated by processing of **P3** or **P4**. Rheological measurements were conducted to provide quantitative information about the mechanical strength (Figure S37-S40). Depending on the storage (G') and loss moduli (G'') as functions of frequency, **P1**, **P2**, **P3**, and **P4** have different rheological performances. Both **P3** and **P4** behavior as liquids, because the values of G'' are always higher than that of G' over the range of frequencies tested (Figure S37).[35,36] Clear transitions from viscoelastic liquids to gel-type solids were observed for **P1** and **P2**, which are in good agreement with the macroscopic observations. **P1** has the highest G' value of 1.6×10^7 Pa at 25 °C, which is considerably higher than that of **P2**, **P3** or **P4** (1-7 orders of magnitude higher (Figure S37). Similar phenomena were observed in the zero-shear viscosity, demonstrating that **P1** is not only mechanically stronger, but also more viscous than **P2**, **P3**, or **P4** (Figure S38). These rheological values are temperature-dependent and dramatically decrease as temperature increases, exhibiting the thermo-sensitive nature of **P1** (Figure S39 and S40).[35-37]

Adhesion properties. **P1** shows excellent adhesion effects on various surfaces, including glass, wood, steel, PTFE, and PMMA. **P1** was first deposited on the surfaces of the substrates, then by gentle heating followed by pressure, **P1** easily coated and adhered to the surfaces (Figure 4c). Water blasting (2 bars, 10 min) could not remove the adhesion layer of **P1** (Figure 1c and movie S3). No tedious solidification processes were required, in comparison to many commercially available glues.[1,2] Using steel as an example, once two pieces of steel were adhered together by **P1**, it was difficult for an external force to separate them. No separation or misplacement was observed in 24 months (0–35 °C, 40–80 RH%) when up to 24 kg was attached to one of the steel pieces (the adhesion area is 15 cm^2, Figure 2a). These macroscopic adhesion tests confirm that the adhesion effect of **P1** is stable and long-term, without occurrence of the attenuated adhesion effect. We previously reported that LMWMs-appended supramolecular adhesives show extremely poor adhesion effects on PTFE and PMMA.[36,37] Here, strong and long-term adhesion on PTFE or PMMA was realized by **P1**. **P1** can easily carry a weight of 8–12

kg without detaching from the adhesion area of PTFE or PMMA (testing for 24 months, adhesion areas are 9–18 cm^2, Figure 2a). The adhesion behavior is closely related to the chemical structures of the supramolecular adhesives, because no adhesion properties were found from **P3** and **P4**. Compared with **P1**, **P2** shows relatively weaker adhesion effects on various surfaces, confirmed by macroscopic adhesion performances. Additional, the adhesion effects of **P2** on surfaces are not as long-acting as that of **P1** (only 1/8 to 1/10 of the adhesion lasting time of **P1**) under the same conditions. No macroscopic adhesion performances were available for **P3** and **P4**.

Lap-shear tests were carried out to quantitatively evaluate the adhesion strengths of **P1**, **P2**, **P3**, and **P4** on different surfaces (Figure 2b).[35,39] The average adhesion strengths of **P1** under ambient conditions (25 °C and 50 RH%) on wood, glass, and steel surfaces are 1.698, 2.017, and 4.174 MPa, respectively, with a pull rate of 100 mm/s. These adhesion values demonstrate that **P1** has strong adhesion performance on hydrophilic surfaces, and shows the best adhesion effect on the steel surface. In comparison to previous supramolecular adhesives, **P1** belongs to the family of

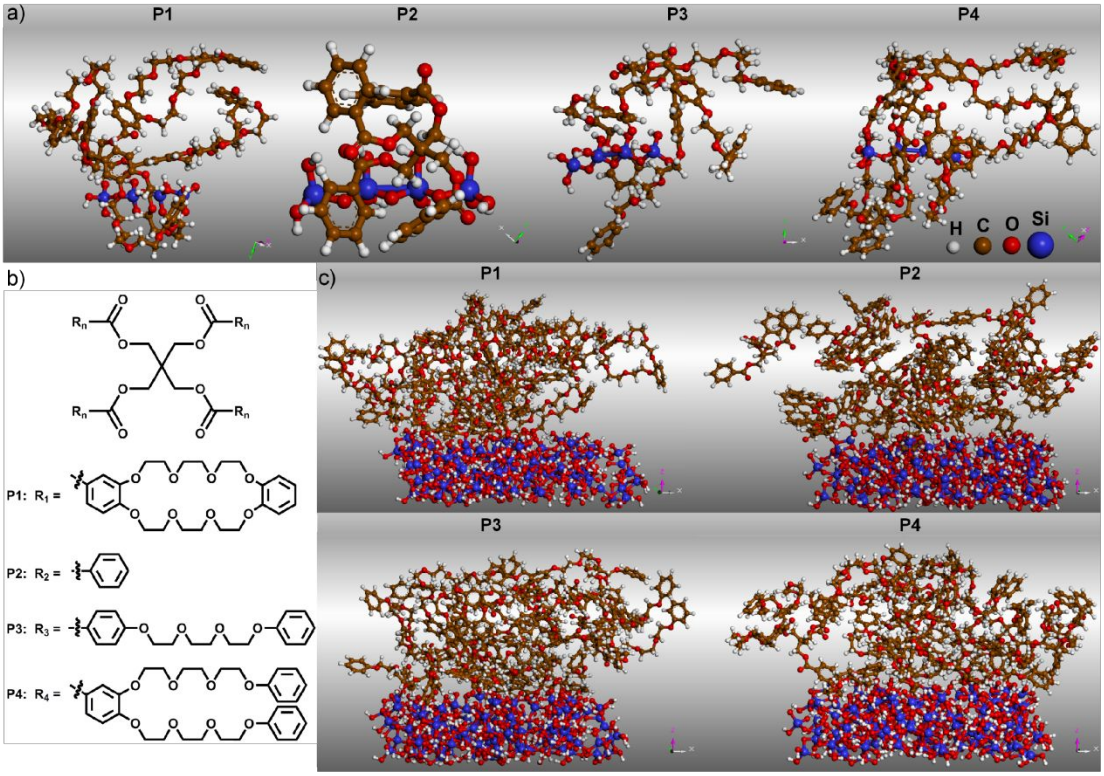

Figure 3. Configurations of molecular models of **P1**-**P4** and glass (with $(HO)_3SiOSi(OH)_2OSi(OH)_3$ as model). a) The interaction mode of individual **P1**-**P4** and glass. b) Chemical structures of **P1**, **P2**, **P3**, and **P4**. c) The most stable state with minimum energy configuration of **P1**-**P4** clusters and glass ($3.0\times3.0\times3.0$ nm^3).

strong adhesives.[1,2] In contrast, **P2** displays weaker adhesion effects on these surfaces. As shown in Figure 2b, the adhesion strengths of **P2**@steel (0.348 MPa) and **P2**@glass (0.725 MPa) are only 1/12 and 1/3 of that of **P1**@steel (4.174 MPa) and **P1**@glass (2.017 MPa), respectively. Compared with the tough adhesion seen on hydrophilic surfaces, the adhesion effect of **P1** on hydrophobic surfaces is relatively weak. An adhesion strength of 0.790 MPa was obtained when **P1** was adhered on a PMMA surface. Weaker adhesion behavior was observed when highly hydrophobic PTFE was used, with an average strength of **P1**@PTFE of 0.277 MPa. Though the adhesion of **P1** on PTFE was not as strong as that of **P1** on hydrophilic surfaces, the adhesion strength of **P1**@PTFE is still much higher than that of many previously reported supramolecular adhesives.[1,2] This is because in most supramolecular adhesion systems, the main adhesion force is hydrogen bonding, which is unfavorable for adhesion onto PTFE. No fatigue and decay of the adhesion effects of **P1** on the five surfaces were observed after multiple cycling tests (10 circulations, Figure 4d). Such excellent reusability can be ascribed to the dynamic and reversible supramolecular interactions of **P1**.[35-37] Almost no adhesion was observed for **P3** and **P4**, as the values of the adhesion strengths are close to the detection limit. By the comparsion of the chemical structures of the four monomers, it can be found that **P2** is rigid, and without flexible crown ether units, which makes **P2** favor aggregation in a dense mode.[40] Based on our previous reported adhesives, the dense aggregated pattern was unfavorable to effective adhesion.[36,37] In addition, the absence of glycol chains leads to weaker interactions between **P2** and surfaces. **P3** and **P4** are oily substances and cannot be solidified during adhesion; neither is suitable for strong adhesion. In shape contrast, **P1** is a viscous liquid during heating and rapidly turns to solid phase after cooling. Such phase transitions indicates **P1** as a good hot molten glue. Meanwhile, closed ring-type crown ether structures of **P1** lead to an extended molecular geometry, which is very different from **P3** and **P4** (flexible glycol chains favor folding together**)**. Such extended structures make it easy to interact with surfaces via supramoelcular interactions (hydrogen bonds, van der Waals interactions, π-π stacking, hydrophobic interactions, even metal-complexation).[1,2,10,36,37] Density Functional Theory (**DFT**)

simulations results further confirmed that among the four monomers, **P1** has the highest combination Gibbs free energy with glass (-51.2 kcal/mol for **P1**, -33.3, -42.7, and -43.6 kcal/mol for **P2**, **P3** and **P4**, respectively) (Figure 3a and Table S5).[41] These results indicate that indiviual **P1** shows the strongest interactions with glass surfaces.

In order to further study the adhesion mechanism between bulky adhesive and glass, the interaction energy between adhesive clusters and glass surfaces was calculated by Molecular Dynamics (**MD**) Simulation. First, a molecular model of the interaction between adhesive and glass was established. In order to simulate the actual contact, the contact cell between adhesive and glass surface was expanded to 3.0×3.0 nm^2. The total thickness was about 3.0 nm. In order to obtain a reasonable interaction configuration between adhesive and glass surface, the molecular model system was followed by geometry optimization, annealing and dynamics balance to obtain the most stable state with minimum energy (Figure 3c).[42,43] Finally, the interaction energy between adhesive and glass was calculated by the following formula at 25 °C and 101 KPa:

$$E_{\text{interfacial}}=E_{\text{total}}-(E_{\text{adhesive}}+E_{\text{glass}}) \quad (1)$$

Here, $E_{\text{interfacial}}$ represents the interaction energy between adhesive and glass surface, and minus means adsorption. E_{adhesive}, E_{glass} are the potential energies of adhesive and glass surface, respectively. E_{total} is the total potential energy of the adhesive-glass system.[42] From the **MD** Simulation, **P1** has the highest interfacial combination energy on glass surfaces (-194.8 kcal/mol for **P1**, -171.3, -176.2, and -189.9 kcal/mol for **P2**, **P3**, and **P4**, respectively) (Table S6). Though **P3** and **P4** have relatively higher interfacial combination energy than that of **P2**, their oily states at 25 °C result in poor adhesion strengths, due to absence of a solidification step (Figure S28 and S29).

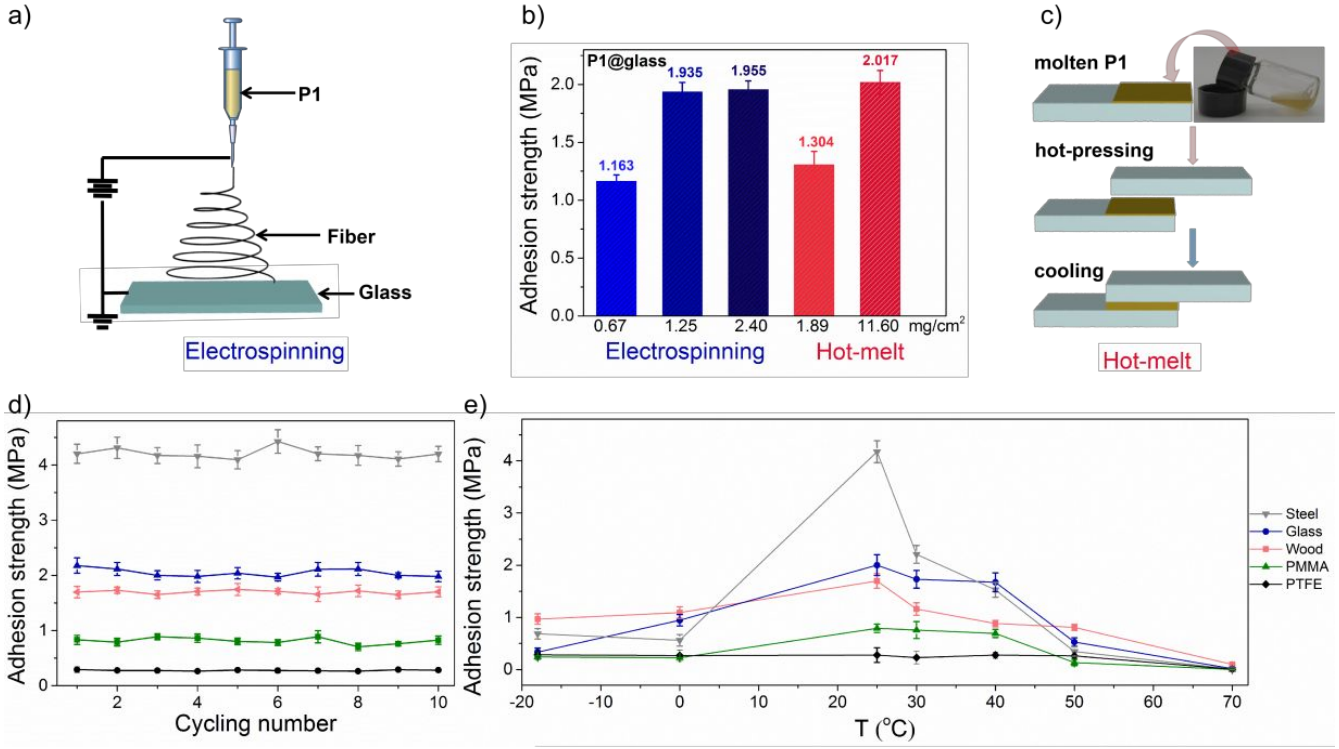

Figure 4. a) Cartoon representations of adhesive coating of **P1** (400 mM, $CHCl_3$) prepared by electrospinning; b) adhesion strengths of **P1** on glass by electrospinning or hot-melt; c) cartoon representations of the adhesion procedure by hot-melt; d) cycling tests of **P1** on different substrates. For all tests, the relative humidity was 50%. For Figure 4b and 4d, temperature was 25 °C; e) Temperature-dependent adhesion strengths of **P1** on different surfaces.

Supramolecular assembly is usually temperature-sensitive, which also affects the adhesion behavior of supramolecular adhesives.[1,2,37,44] According to the temperature-dependent lap-shear tests, it is obvious that high temperature is harmful to the adhesion effect, as depicted in Figure 4e and Table S1. No obvious adhesion was observed when the temperature reached 70 °C for all surfaces tested. Low temperature was also shown to reduce the adhesion strengths. For example, when the temperature was kept at -18 °C, the adhesion strength of **P1**@wood is about half of that at 25 °C (0.967 MPa at -18 °C and 1.697 MPa at 25 °C). In general, the adhesion effect of **P1** is more sensitive to high temperature than to low temperature. **P1**@PTFE is the least sensitive to elevated temperature. When the temperature was increased from 25 °C to 50 °C, **P1**@PTFE maintained 94% adhesion strength (0.277 MPa at 25 °C and 0.261 MPa at 50 °C). By comparing the adhesion strengths of **P1** on different surfaces at 25 °C and 50 °C, **P1**@glass, **P1**@wood, **P1**@PMMA, and **P1**@steel, only retained 30.3%, 47.5%, 16.7%, and 8.2% adhesion strengths, respectively. For all surfaces tested in this study, 25 °C is the optimal temperature for the adhesion effect of **P1**. These temperature-dependent adhesion results are consistent with the rheological measurements and macroscopic tests (Figure 4e, S39, and S40).

Supramolecular adhesion by electrospinning. Coating adhesive materials homogeneously on surfaces is a key step to realize highly effective adhesion.[1,2,18-20] Usually adhesive materials are hand-mounted on surfaces, which causes two main problems: it is difficult to get a uniform adhesion layer and leads to a waste of adhesive materials. Electrospinning has been recognized as a low-cost but highly effective technique for the preparation of polymer fibers with uniform size.[45-47] However,

electrospinning is rarely applied in the fabrication of supramolecular adhesion coatings. **P1** was successfully coated onto a glass surface by electrospinning (Figure S24). As shown in Figure 4b, a very small amount of **P1** (1.935 MPa, 1.25 mg/cm^2) can give a strong adhesion effect, compared with the hand-mounting method (2.017 MPa, 11.6 mg/cm^2). When the amount of **P1** was reduced even further to 0.67 mg/cm^2, a moderate adhesion strength was still achieved (1.163 MPa). More importantly, the adhesive coating process by electrospinning is remarkably time-saving. For example, when coating an area of 20×20 cm^2, it takes more than one hour to prepare a uniform coating layer of **P1**. In contrast, one minute is enough to obtain a more uniform coating layer of **P1** by electrospining. This electrospining method provides savings not only in the adhesive materials, but also in time, human cost, and energy.

Water-resistant and underwater adhesion performances. Adhesion in a high-moisture environment, or even under water is important for the practical applications of adhesive materials.[10-15] Up until now, tough adhesion on wet surfaces has been a challenge for supramolecular adhesives, due to the water-induced instabilities of supramolecular adhesive structures and their adhesion capacities.[10,18-20] Adhesion tests of **P1** at different humidity conditions were carried out. To our delight, **P1** displays excellent adhesion performances in high-moisture environments. As shown in Figure 5a, when the RH was increased from 5% to 95%, only very slight losses (0.3−8.4%) of the adhesion strengths of **P1** on different surfaces were observed. Long-term experiments further confirmed the water-insensitive properties of **P1** when adhered on different surfaces. After storage in a high-moisture environment (95 RH%) for 24 months (two glass plates adhered

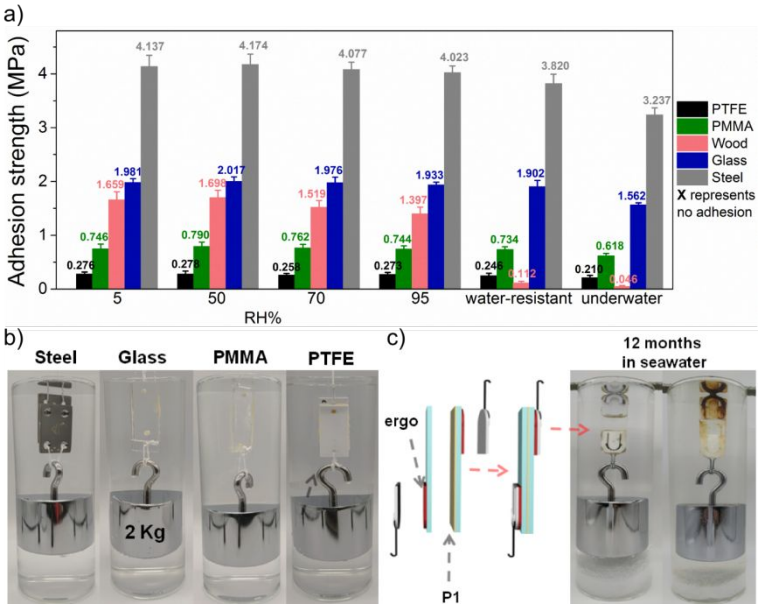

Figure 5. a) The adhesion strengths of **P1** on different substrates at different humidity or under water; b) water-resistant adhesion of **P1** on different surfaces; c) cartoon representations and macroscopic views of the adhesion process of **P1** in seawater for 12 months. In Figure 5c, commercially available glue ergo was used to adhere the hooks and **P1** was used to adhere two glass plates. During the whole test process, hooks fell off from the glass plates six times, while two glass plates were still adhered firmly. All tests were carried out at 25 °C.

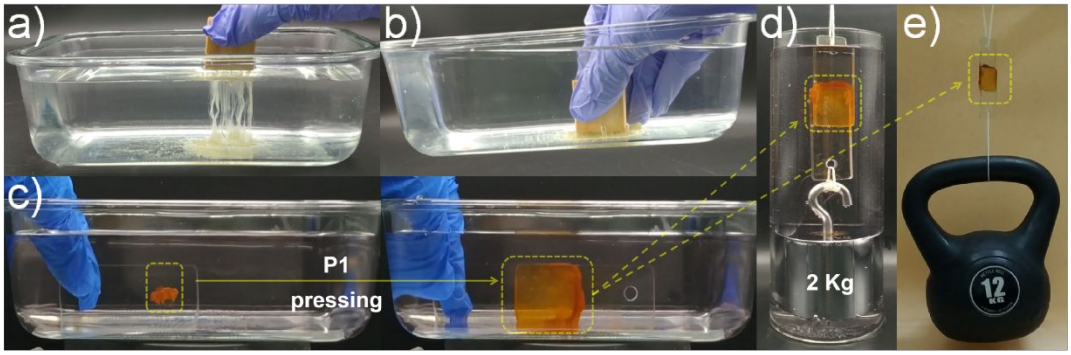

Figure 6. Underwater adhesion of **P1**: a,b) a wooden block and a glass container adhered by **P1** under water; c) underwater adhesion process of **P1** and macroscopic test of the underwater adhesion behavior of **P1** in water or in air. For Figure 6c, a red dye was mixed with **P1** to get a clear view.

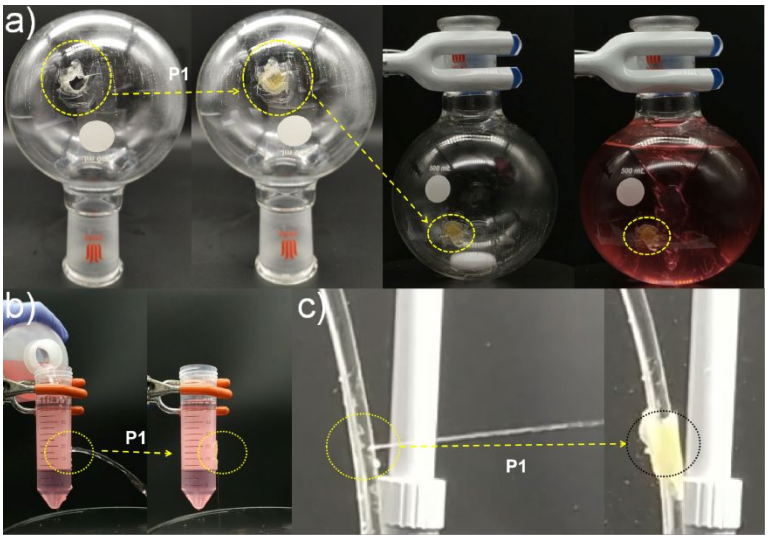

Figure 7. Applications of **P1**: a) round bottom flask repaired by **P1**; b) a centrifuge tube repaired by **P1**; c) a water pipe repaired by **P1**.

by **P1**), neither attenuated adhesion effects nor decreased adhesion strengths were observed. In contrast, when **P1** was replaced by **P2**, decreased adhesion strengths were measured (decrease of 40−60%, compared with the adhesion strengths of **P2** at 50 RH%).

Based on the positive results of the adhesion behavior of **P1** in high-moisture environments, we later explored the water-resistant and underwater adhesion properties of **P1** on different surfaces. For the water-resistant tests, adhesion samples were prepared anhydrously, and these samples were placed in water for 24 hours before lap-shear testing. Less than a 10% loss in the adhesion strengths were observed, in comparison with that of water-free samples (Figure 5a). For example, the adhesion strengths of **P1**@glass and **P1**@steel (25 °C, 50 RH%) are 2.017 and 4.174 MPa, while the adhesion strengths of **P1**@glass and **P1**@steel (placed in water for 24 hours) are 1.902 and 3.820 MPa, respectively. Time-dependent adhesion tests demonstrate that **P1** still has excellent water-resistant adhesion effects, even in samples that were treated with water for 12 months. Macroscopic tests further confirmed the water-resistant adhesion effects of **P1** on different surfaces, which are presented in Figure 5b. After hanging a weight of 2 kg for 12 months, no displacement or separation occurred. A bridge prepared by three PMMA building blocks can carry more than 65 kg in water (Figure S41 and movie S4). Such water-resistant adhesion behavior was not merely realized in water, but also in seawater (containing 3.5 wt% NaCl), which expands the application of **P1** as a marine adhesive (Figure 5c).[19]

Following on from the results of **P1** as a water-resistant adhesive, the underwater adhesion properties of **P1** were investigated further (Figure 6). Using adhesion on glass as an example, **P1** was first coated on the surface of a glass plate under water, then a new glass plate was placed on top (Figure 6c and movie S5). After pressing for 10 min, **P1**@glass was placed under water for 24 hours before lap-shear testing. The underwater adhesion strengths of **P1** on five surfaces are plotted in Figure 5a. The underwater adhesion strengths of **P1**@glass, **P1**@steel, and **P1**@PMMA are as high as 1.562, 3.237, and 0.618 MPa, respectively. Though the underwater adhesion is not as strong as the water-free or water-resistant adhesion, the values of underwater adhesion strengths are still high compared to previously reported underwater adhesives. **P1** failed to effectively adhere wood together when placed under water for more than 24 hours; however, short-term (0.5 to 1 hour) underwater adhesion of **P1** on wood is feasible (Figure 6a,b, Table S3, and movie S6). This weak underwater adhesion of **P1** on wood can be ascribed to the porous structure of the wood surface, which can form a water layer between **P1** and the wood surface, thus destroying the adhesion capacity of **P1**. No underwater adhesion properties were observed from **P2**, **P3**, **P4**, and some commercial adhesives (Table S4). Compared with catechol-based bioadhesives, **P1** is a strong underwater adhesive and represents a new type of supramolecular adhesive without the polymeric backbones and catechol units.[11,31,48] For example, the underwater adhesive reported by Wilker reached an adhesion strength of 3.000 MPa,[23] and here the underwater adhesion strength of **P1** is comparable (3.237 MPa).

With the water-resistant and underwater adhesion performances of **P1** in mind, application tests of **P1** were carried out (Figure 7). **P1** was successfully used as a water-resistant adhesive to repair broken flasks, as shown in Figure 7a and movie S7. After using the repaired flask for 12 months (with water, 25 °C), the **P1** patch was still firmly adhered to the leak of the flask. The leakage of water pipes is a common occurrence in daily life. An adhesive for the leakage of water pipes needs strong, fast, and long-term adhesion effects. Based on the advantages of **P1**, broken pipes with water blast (2 bars) can be easily and instantly repaired by **P1** (Figure 7c and movie S10).

CONCLUSIONS

In conclusion, herein we have reported a new supramolecular adhesive material based on LMWMs. Versatile and tough adhesion of **P1** on different surfaces was successfully realized. Underwater and water-resistant adhesion of **P1** with stable and long-term adhesion performances were also shown. The long-term adhesion effect in seawater further extends the potential application of **P1** as a marine adhesive. The application of electrospinning in the supramolecular adhesive field represents a facile and economical method to prepare supramolecular adhesive coatings. We hope that supramolecular adhesive materials consisting of LMWMs would offer great potential in the research fields of biodegradable adhesives, tissue repair, and surface adhesion.

ASSOCIATED CONTENT

Supporting Information

The Supporting Information is available free of charge on the ACS Publications website.

Experimental procedures, characterization and NMR spectra for obtained compounds and other materials (PDF).

AUTHOR INFORMATION

Corresponding Author

* dongsy@hnu.edu.cn
* zhaogai@nuaa.edu.cn

ORCID

Shengyi Dong: 0000-0002-8640-537X

Notes

The authors declare no competing financial interests.

ACKNOWLEDGMENT

This work was supported by National Natural Science Foundation of China (21704024), Huxiang Young Talent Program from Hunan Province (2018RS3036), and the Fundamental Research Funds for the Central Universities from Hunan University.

REFERENCES

(1) Heinzmann, C.; Weder, C.; de Espinosa, L. M. Supramolecular Polymer Adhesives: Advanced Materials Inspired by Nature. *Chem. Soc. Rev.* **2016**, *45*, 342–358.

(2) Ji, X.; Ahmed, M.; Long, L.; Khashab, N. M.; Huang, F.; Sessler, J. L. Adhesive Supramolecular Polymeric Materials Constructed from Macrocycle-Based Host-Guest Interactions. *Chem. Soc. Rev.* **2019**, *48*, 2682–2697.

(3) Gao, Z.; Yue, C.; Cao, H.; Wang, X.; Zhu, X.; Lin, R. Preparation and Formaldehyde Emission and Bonding Performance of Novel Modified Urea-Formaldehyde Resin Adhesive. *Adv. Mater. Res.* **2012**, *490–495*, 3476–3480.

(4) Zhu, Y.; Di, B.; Chen, H.; Wang, X.; Tian, Y. In Situ Synthesis of Novel Biomass Lignin/Silica Based Epoxy Resin Adhesive from Renewable Resources at Different pHs. *J. Adhes. Sci. Technol.* **2019**, *33*, 1806–1820.

(5) Parija, S.; Misra, M.; Mohanty, A. K. Studies of Natural Gum Adhesive Extracts: an Overview. *J. Macromol. Sci., Polym. Rev.* **2001**, *41*, 175–197.

(6) Kim, J. H.; Min, H. J.; Park, K.; Kim, J. Preparation and Evaluation of a Cosmetic Adhesive Containing Guar Gum. *Korean J. Chem. Eng.* **2017**, *34*, 2236–2240.

(7) Liu, J.; Scherman, O. A. Cucurbit[n]uril Supramolecular Hydrogel Networks as Tough and Healable Adhesives. *Adv. Funct. Mater.* **2018**, *28*, 1800848.

(8) Zhang, F.; Xiong, L.; Ai, Y.; Liang, Z.; Liang, Q. Stretchable Multiresponsive Hydrogel with Actuatable, Shape Memory, and Self-Healing Properties. *Adv. Sci.* **2018**, *5*, No. 1800450.

(9) Gan, D.; Xing, W.; Jiang, L.; Fang, J.; Zhao, C.; Ren, F.; Fang, L.; Wang, K.; Lu, X. Plant-Inspired Adhesive and Tough Hydrogel Based on Ag-Lignin Nanoparticles-Triggered Dynamic Redox Catechol Chemistry. *Nat. Commun.* **2019**, *10*, 1487–1497.

(10) Yang, J.; Bai, R.; Chen, B.; Suo, Z. Hydrogel Adhesion: A Supramolecular Synergy of Chemistry, Topology, and Mechanics. *Adv. Funct. Mater.* **2020**, *30*, 1901693.

(11) Stewart, R. J.; Ransom, T. C.; Hlady, V. Natural Underwater Adhesives. *J. Polym. Sci. B* **2011**, *49*, 757–771.

(12) Stewart, R. J. Protein-Based Underwater Adhesives and the Prospects for Their Biotechnological Production. *Appl. Microbiol. Biotechnol.* **2011**, *89*, 27–33.

(13) Ahn, Y.; Jang, Y.; Selvapalam, N.; Yun, G.; Kim, K. Supramolecular Velcro for Reversible Underwater Adhesion. *Angew. Chem., Int. Ed.* **2013**, *52*, 3140–3144.

(14) Xu, J.; Li, X.; Li, X.; Li, B.; Wu, L.; Li, W.; Xie, X.; Xue, R. Supramolecular Copolymerization of Short Peptides and Polyoxometalates: toward the Fabrication of Underwater Adhesives. *Biomacromolecules* **2017**, *18*, 3524–3530.

(15) Yang, J.; Bai, R.; Suo, Z. Topological Adhesion of Wet Materials. *Adv. Mater.* **2018**, *30*, 1800671.

(16) Matos-Pérez, C. R.; White, J. D.; Wilker, J. J. Polymer Composition and Substrate Influences on the Adhesive Bonding of a Biomimetic, Cross-Linking Polymer. *J. Am. Chem. Soc.* **2012**, *134*, 9498–9505.

(17) Seo, S.; Das, S.; Zalicki, P. J.; Mirshafian, R.; Eisenbach, C. D.; Israelachvili, J. N.; Waite, J. H.; Ahn, B. K. Microphase Behavior and Enhanced Wet-Cohesion of Synthetic Copolyampholytes Inspired by a Mussel Foot Protein. *J. Am. Chem. Soc.* **2015**, *137*, 9214−9217.

(18) Ahn, B. K. Perspectives on Mussel-Inspired Wet Adhesion. *J. Am. Chem. Soc.* **2017**, *139*, 10166−10171.

(19) Hofman, A. H.; van Hees, I. A.; Yang, J.; Kamperman, M. Bioinspired Underwater Adhesives by Using the Supramolecular Toolbox. *Adv. Mater.* **2018**, *30*, 1704640.

(20) Pinnaratip, R.; Bhuiyan, M. S. A.; Meyers, K.; Rajachar, R. M.; Lee, B. P. Multifunctional Biomedical Adhesives. *Adv. Healthcare Mater.* **2019**, *8*, 1801568.

(21) Degen, G. D.; Stow, P. R.; Lewis, R. B.; Eguiluz, R. C. A.; Valois, E.; Kristiansen, K.; Butler, A.; Israelachvili, J. N. Impact of Molecular Architecture and Adsorption Density on Adhesion of Mussel-Inspired Surface Primers with Catechol-Cation Synergy. *J. Am. Chem. Soc.* **2019**, *141*, 18673−18681.

(22) Wilker, J. J. Self-Healing Polymers: Sticky when Wet. *Nat. Mater.* **2014**, *13*, 849–850.

(23) North, M. A.; Del Grosso, C. A.; Wilker, J. J. High Strength Underwater Bonding with Polymer Mimics of Mussel Adhesive Proteins. *ACS Appl. Mater. Interfaces* **2017**, *9*, 7866−7872.

(24) Shao, H.; Stewart, R. J. Biomimetic Underwater Adhesives with Environmentally Triggered Setting Mechanisms. *Adv. Mater.* **2010**, *22*, 729–733.

(25) Jones, J. P.; Sima, M.; O'Hara, R. G.; Stewart, R. J. Water-Borne Endovascular Embolics Inspired by the Undersea Adhesive of Marine Sandcastle Worms. *Adv. Healthcare Mater.* **2016**, *5*, 795–801.

(26) Xu, Y.; Liu, Q.; Narayanan, A.; Jain, D.; Dhinojwala, A.; Joy, A. Mussel-Inspired Polyesters with Aliphatic Pendant Groups Demonstrate the Importance of Hydrophobicity in Underwater Adhesion. *Adv. Mater. Interfaces* **2017**, *4*, 1700506.

(27) Narayanan, A.; Kaur, S.; Peng, C.; Debnath, D.; Mishra, K.; Liu, Q.; Dhinojwala, A.; Joy, A. Viscosity Attunes the Adhesion of Bioinspired Low Modulus Polyester Adhesive Sealants to Wet Tissues. *Biomacromolecules* **2019**, *20*, 2577–2586.

(28) Lee, B. P.; Konst, S. Novel Hydrogel Actuator Inspired by Reversible Mussel Adhesive Protein Chemistry. *Adv. Mater.* **2014**, *26*, 3415–3419.

(29) Narkar, A. R.; Barker, B.; Clisch, M.; Jiang, J.; Lee, B. P. pH Responsive and Oxidation Resistant Wet Adhesive Based on Reversible Catechol-Boronate Complexation. *Chem. Mater.* **2016**, *28*, 5432–5439.

(30) Courtois, J.; Baroudi, I.; Nouvel, N.; Degrandi, E.; Pensec, S.; Ducouret, G.; Chanéac, C.; Bouteiller, L.; Creton, C. Supramolecular Soft Adhesive Materials. *Adv. Funct. Mater.* **2010**, *20*, 1803–1811.

(31) Maier, G. P.; Rapp, M. V.; Waite, J. H.; Israelachvili, J. N.; Butler, A. Adaptive Synergy between Catechol and lysine Promotes Wet Adhesion by Surface Salt Displacement. *Science* **2015**, *349*, 628–632.

(32) Wu, Z.; Ji, C.; Zhao, X.; Han, Y.; Müllen, K.; Pan, K.; Yin, M. Green-Light-Triggered Phase Transition of Azobenzene Derivatives toward Reversible Adhesives. *J. Am. Chem. Soc.* **2019**, *141*, 7385–7390.

(33) Niu, Z.; Gibson, H. W. Polycatenanes. *Chem. Rev.* **2009**, *109*, 6024–6046.

(34) Zhou, H.; Xue, C.; Weis, P.; Suzuki, Y.; Huang, S.; Koynov, K.; Auernhammer, G. K.; Berger, R.; Butt, H.-J.; Wu, S. Photoswitching of Glass Transition Temperatures of Azobenzene-Containing Polymers Induces Reversible Solid-to-Liquid Transitions. *Nat. Chem.* **2017**, *9*, 145–151.

(35) Zhang, Q.; Shi, C.-Y.; Qu, D-H.; Long, Y.-T.; Feringa, B. L.; Tian, H. Exploring a Naturally Tailored Small Molecule for Stretchable, Self-Healing, and Adhesive Supramolecular Polymers. *Sci. Adv.* **2018**, *4*, No. eaat8192.

(36) Dong, S.; Leng, J.; Feng, Y.; Liu, M.; Stackhouse, C. J.; Schönhals, A.; Chiappisi, L.; Gao, L.; Chen, W.; Shang, J.; Jin, L.; Qi, Z.; Schalley, C.

A. Structural Water as an Essential Comonomer in Supramolecular Polymerization. *Sci. Adv.* **2017**, *3*, No. eaao0900.

(37) Zhang, Q.; Li, T.; Duan, A.; Dong, S.; Zhao, W.; Stang, P. J. Formation of a Supramolecular Polymeric Adhesive via Water-Participant Hydrogen Bond Formation. *J. Am. Chem. Soc.* **2019**, *141*, 8058–8063.

(38) Rapp, M. V.; Maier, G. P.; Dobbs, H. A.; Higdon, N. J.; Waite, J. H.; Butler, A.; Israelachvili, J. N. Defining the Catechol—Cation Synergy for Enhanced Wet Adhesion to Mineral Surfaces. *J. Am. Chem. Soc.* **2016**, *138*, 9013−9016.

(39) Anderson, C. A.; Jones, A. R.; Briggs, E. M.; Novitsky, E. J.; Kuykendall, D. W.; Sottos, N. R.; Zimmerman, S. C. High-Affinity DNA Base Analogs as Supramolecular, Nanoscale Promoters of Macroscopic Adhesion. *J. Am. Chem. Soc.* **2013**, *135*, 7288–7295.

(40) Nättinen, K. I.; Rissanen, K. Dendritic Pyridine-Functionalized Polyesters and Their Polycationic Hydrogen Bonded Picrates: Synthesis and X-ray Structural Study of Weak Hydrogen Bonding. *Crystal Growth & Design* **2003**, *3*, 339–353.

(41) Bannwarth, C.; Ehlert, S.; Grimme, S. GFN2-xTB—An Accurate and Broadly Parametrized Self-Consistent Tight-Binding Quantum Chemical Method with Multipole Electrostatics and Density-Dependent Dispersion Contributions. *J. Chem. Theory Comput.* **2019**, *15*, 1652–1671.

(42) Sun, H. COMPASS: An ab Initio Force-Field Optimized for Condensed-Phase Applicationss Overview with Details on Alkane and Benzene Compounds. *J. Phys. Chem. B* **1998**, *102*, 7338–7364.

(43) Li, Y.; Wang, S.; Wang, Q. A Molecular Dynamics Simulation Study on Enhancement of Mechanical and Tribological Properties of Polymer Composites by Introduction of Graphene. *Carbon* **2017**, *111*, 538–545.

(44) Dompé, M.; Cedano-Serrano, F. J.; Heckert, O.; van den Heuvel, N.; van der Gucht, J.; Tran, Y.; Hourdet, D.; Creton, C.; Kamperman, M. Thermoresponsive Complex Coacervate-Based Underwater Adhesive. *Adv. Mater.* **2019**, *31*, 1808179.

(45) Yan, X.; Zhou, M.; Chen, J.; Chi, X.; Dong, S.; Zhang, M.; Ding, X.; Yu, Y.; Shao, S.; Huang, F. Supramolecular Polymer Nanofibers via Electrospinning of a Heteroditopic Monomer. *Chem. Commun.* **2011**, *47*, 7086–7088.

(46) Wang, K.; Wang, C.-Y.; Wang, Y.; Li, H.; Bao, C.-Y.; Liu, J.-Y.; Zhang, S. X.-A.; Yang, Y.-W. Electrospun Nanofibers and Multi-Responsive Supramolecular Assemblies Constructed from a Pillar[5]arene-Based Receptor. *Chem. Commun.* **2013**, *49*, 10528–10530.

(47) Wang, X.; Han, Y.; Liu, Y.; Zou, G.; Gao, Z.; Wang, F. Cooperative Supramolecular Polymerization of Fluorescent Platinum Acetylides for Optical Waveguide Applications. *Angew. Chem., Int. Ed.* **2017**, *56*, 12466–12470.

(48) Zhao, Q.; Lee, D. W.; Ahn, B. K.; Seo, S.; Kaufman, Y.; Israelachvili, J. N.; Waite, J. H. Underwater Contact Adhesion and Microarchitecture in Polyelectrolyte Complexes Actuated by Solvent Exchange. *Nat. Mater.* **2016**, *15*, 407–412.

Toc:

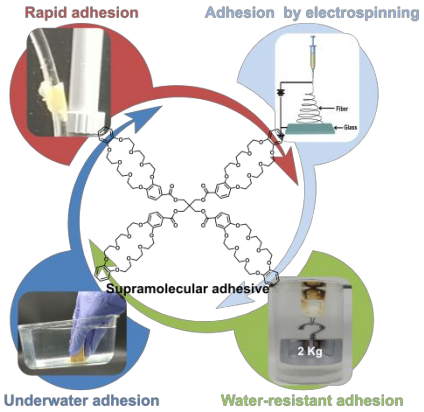

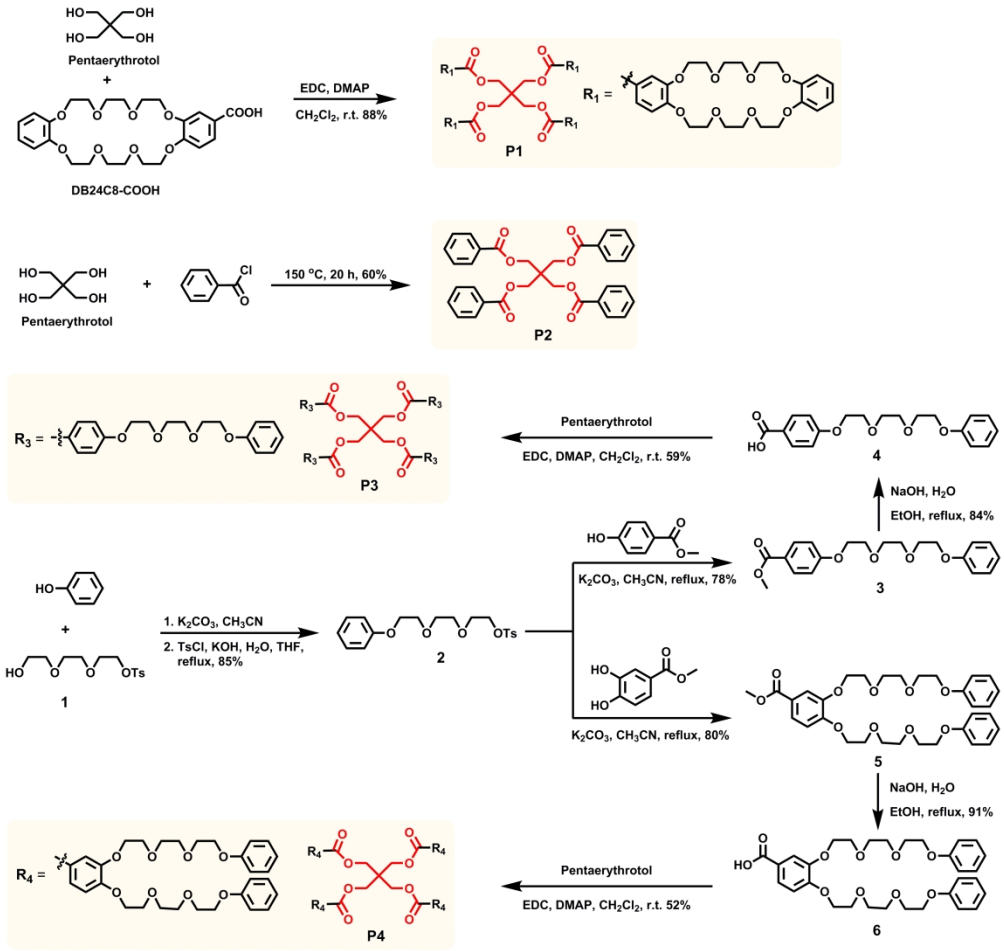

Scheme 1

284x270mm (300 x 300 DPI)

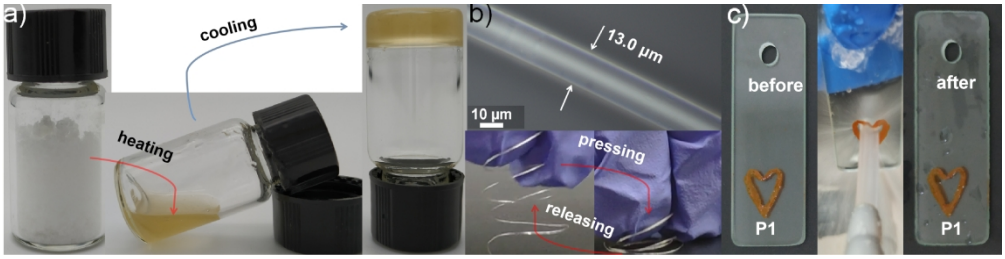

Figure 1

1131x284mm (96 x 96 DPI)

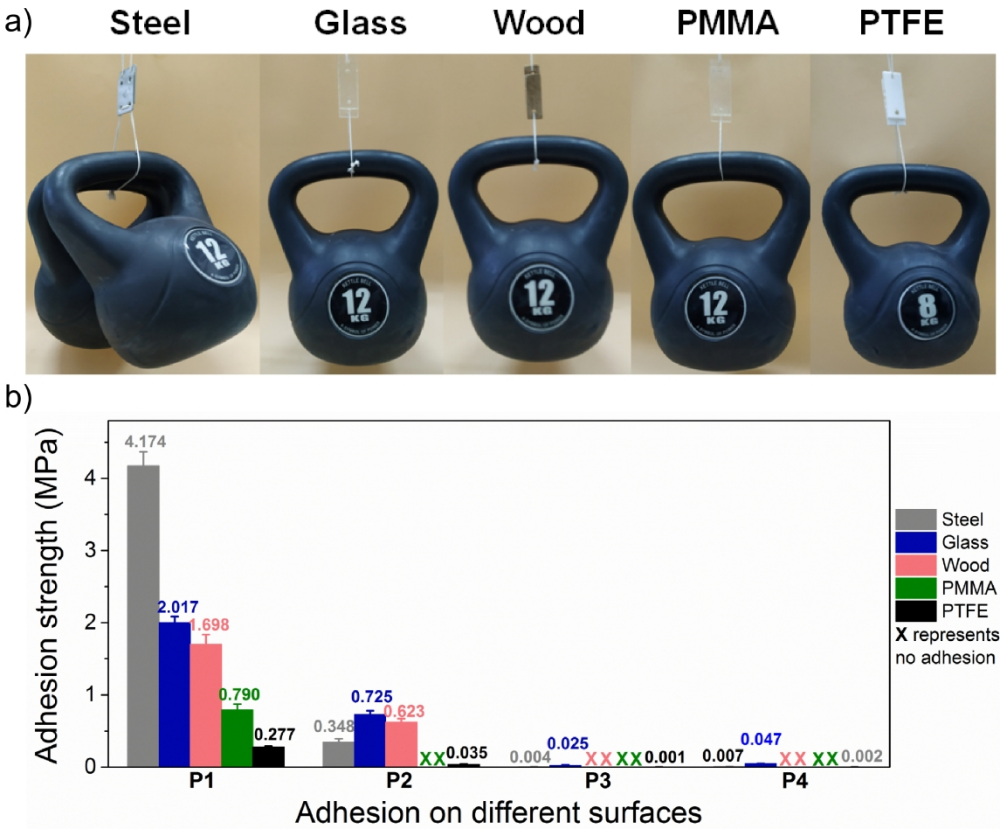

Figure 2

899x738mm (96 x 96 DPI)

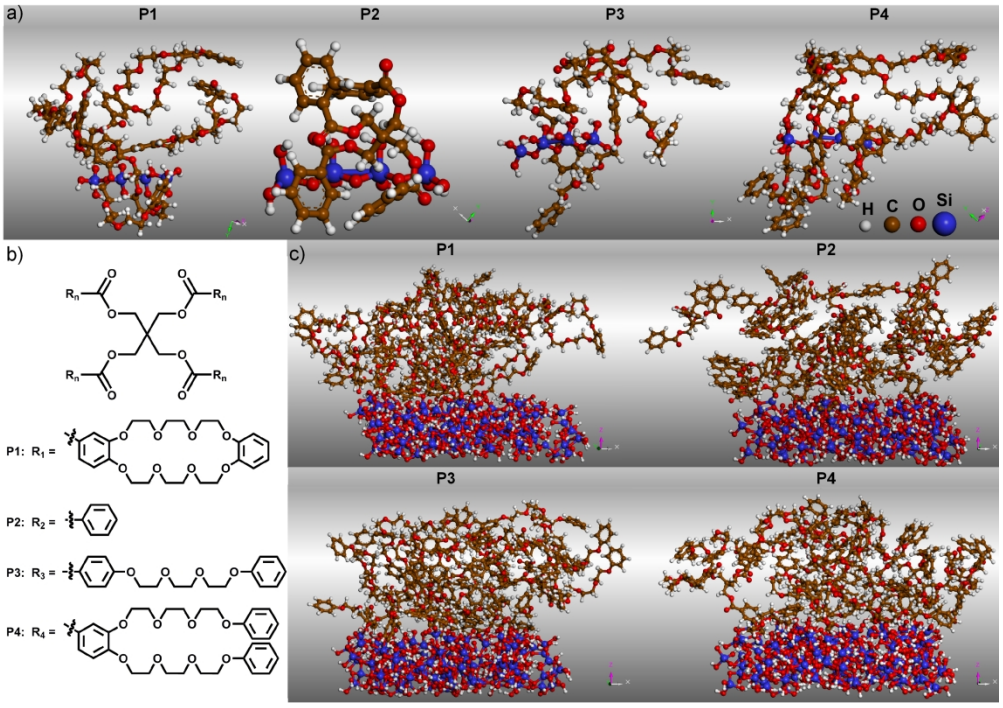

Figure 3

894x625mm (96 x 96 DPI)

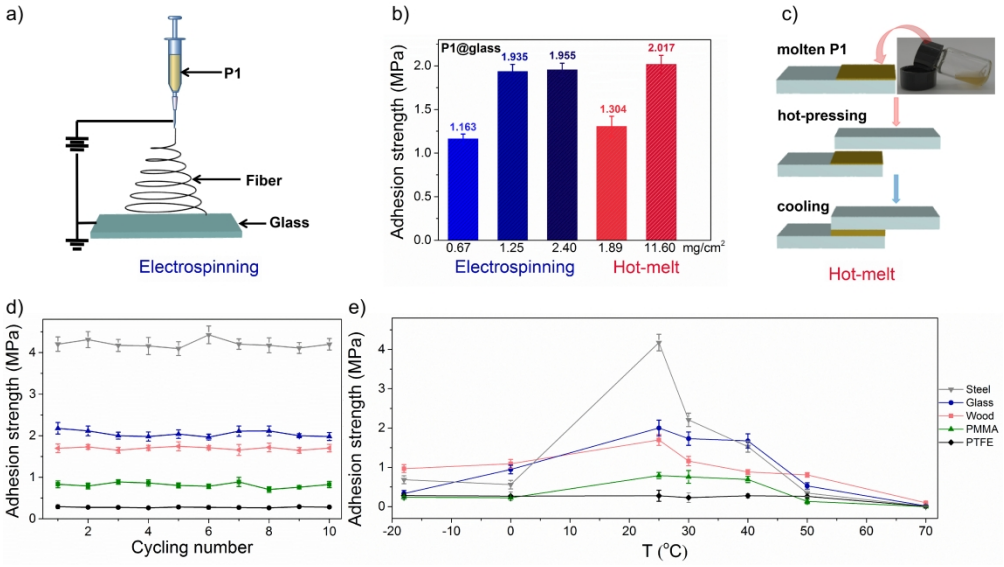

Figure 4

1341x758mm (96 x 96 DPI)

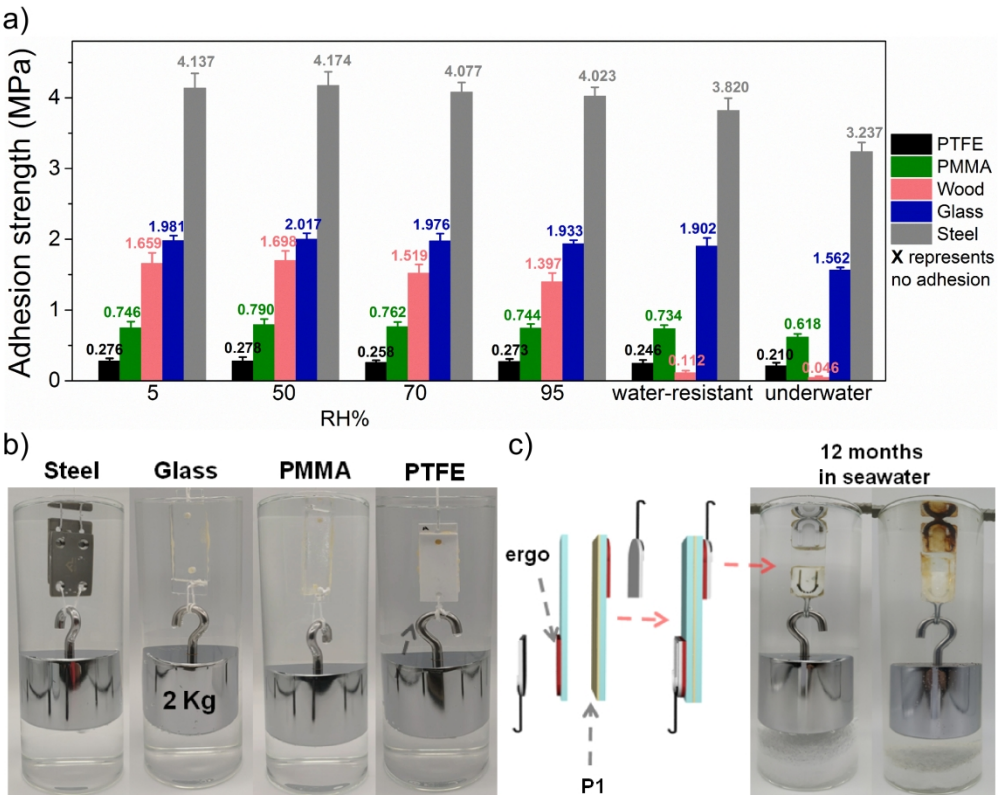

Figure 5

883x704mm (96 x 96 DPI)

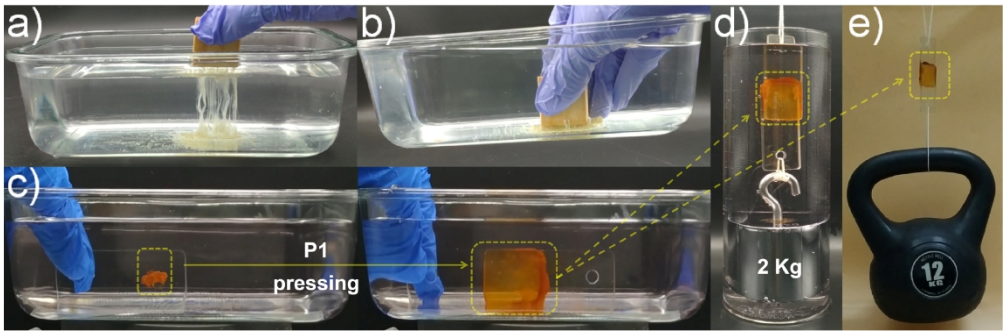

Figure 6

900x294mm (96 x 96 DPI)

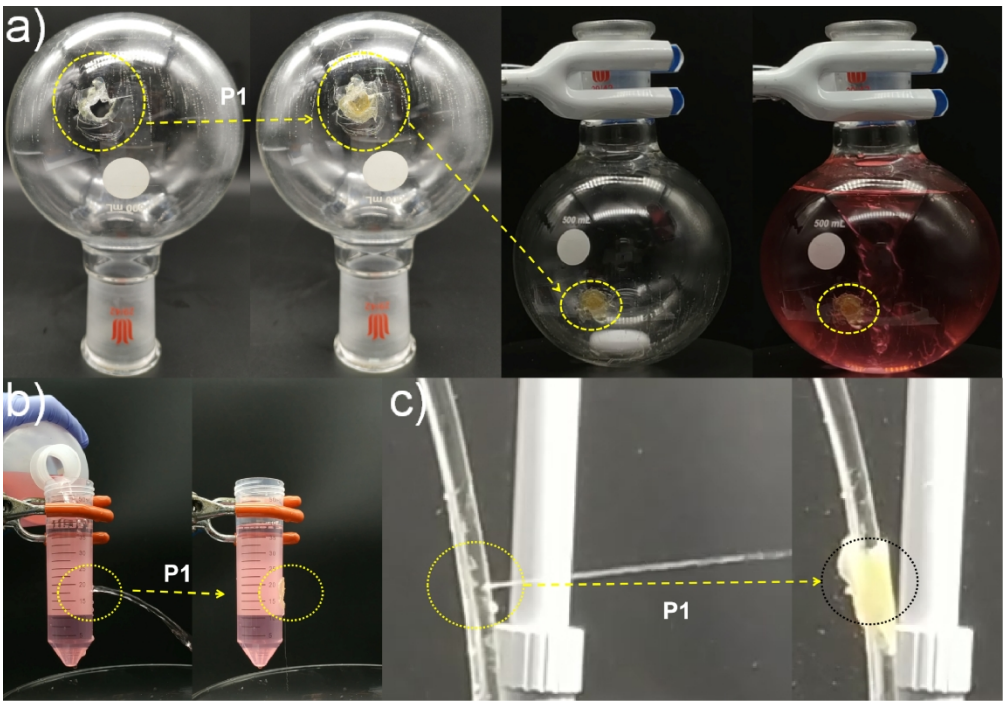

Figure 7

870x603mm (96 x 96 DPI)

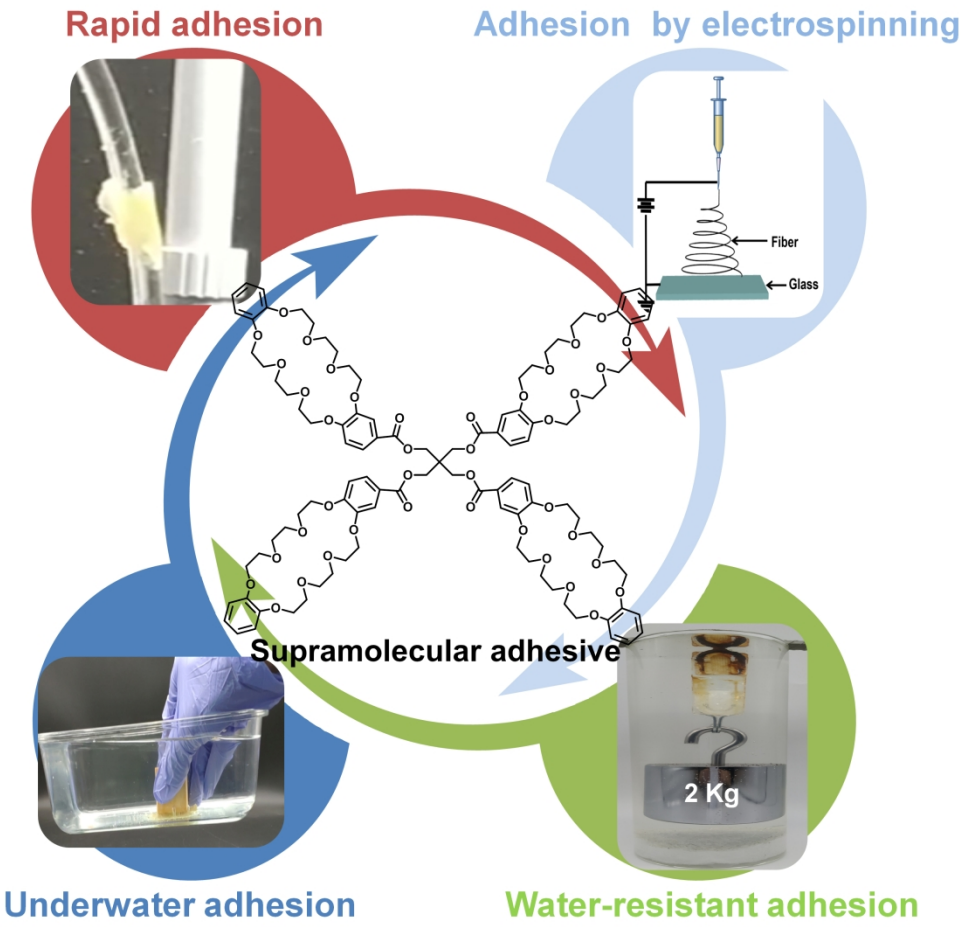

Toc graphic

761x712mm (96 x 96 DPI)